Journal of Hydrology 482 (2013) 57–68

Contents lists available at SciVerse ScienceDirect

Journal of Hydrology

journal homepage: www.elsevier.com/locate/jhydrol

Trend analysis of runoff and sediment fluxes in the Upper Blue Nile basin: A combined analysis of statistical tests, physically-based models and landuse maps

T.G. Gebremicael [a,*], Y.A. Mohamed [a,b,c], G.D. Betrie [d], P. van der Zaag [a,b], E. Teferi [a,e]

[a] UNESCO-IHE, Institute for Water Education, P.O. Box 3015, 2601 DA Delft, The Netherlands
[b] Delft University of Technology, P.O. Box 5048, 2600 GA Delft, The Netherlands
[c] Hydraulic Research Station, P.O. Box 318, Wad Medani, Sudan
[d] School of Engineering, University of British Columbia, Kelowna, BC, Canada V1V 1V7
[e] College of Development Studies, Addis Ababa University, P.O. Box 2176, Ethiopia

ARTICLE INFO

Article history:
Received 1 October 2012
Received in revised form 3 December 2012
Accepted 15 December 2012
Available online 26 December 2012
This manuscript was handled by Konstantine P. Georgakakos, Editor-in-Chief, with the assistance of Ashish Sharma, Associate Editor

Keywords:
Blue Nile
SWAT
Statistical analysis
Runoff flux
Sediment flux

SUMMARY

The landuse/cover changes in the Ethiopian highlands have significantly increased the variability of runoff and sediment fluxes of the Blue Nile River during the last few decades. The objectives of this study were (i) to understand the long-term variations of runoff and sediment fluxes using statistical models, (ii) to interpret and corroborate the statistical results using a physically-based hydrological model, Soil and Water Assessment Tool (SWAT), and (iii) to validate the interpretation of SWAT results by assessing changes of landuse maps. Firstly, Mann–Kendall and Pettitt tests were used to test the trends of Blue Nile flow (1970–2009) and sediment load (1980–2009) at the outlet of the Upper Blue Nile basin at El Diem station. These tests showed statistically significant increasing trends of annual stream flow, wet season stream flow and sediment load at 5% confidence level. The dry season flow showed a significant decrease in the trend. However, during the same period the annual rainfall over the basin showed no significant trends. The results of the statistical tests were sensitive to the time domain. Secondly, the SWAT model was used to simulate the runoff and sediment fluxes in the early 1970s and at the end of the time series in 2000s in order to interpret the physical causes of the trends and corroborate the statistical results. A comparison of model parameter values between the 1970s and 2000s shows significant change, which could explain catchment response changes over the 28 years of record. Thirdly, a comparison of landuse maps of 1970s against 2000s shows conversion of vegetation cover into agriculture and grass lands over wide areas of the Upper Blue Nile basin. The combined results of the statistical tests, the SWAT model, and landuse change detection are consistent with the hypothesis that landuse change has caused a significant change of runoff and sediment load from the Upper Blue Nile during the last four decades. This is an important finding to inform optimal water resources management in the basin, both upstream in the Ethiopian highlands, and further downstream in the plains of Sudan and Egypt.

1. Introduction

The Upper Blue Nile River basin contributes over 60% of the Nile's water (Conway, 2000). It is crucial for the socio-economic development and environmental stability of the three riparian countries, which are Ethiopia, Sudan and Egypt. However, landuse/cover and climate changes have affected the value of the Blue Nile's water through increasing inter-annual and inter-decadal variability of runoff and sediment fluxes (Conway et al., 2004; Hurni et al., 2005). These changes have resulted in a negative impact in both the upstream and downstream countries. In the Ethiopian highlands, landuse change has led to severe soil erosion, which reduced the soil moisture holding capacity and challenged food production (Hurni, 1993; Tibebe and Bewket, 2010). On the other hand, the downstream countries (i.e., Sudan and Egypt) have experienced serious problems in their storage reservoirs and irrigation canals due to the excessive sediment loads (NBCBN, 2005; Garzanti et al., 2006; Easton et al., 2010; Betrie et al., 2011).

A literature review shows that there are many local and basin level studies in the Blue Nile's flow. The long-term trend analysis of runoff was studied by Conway and Hulme (1993), Legesse et al. (2003), Bewket (2003), Gebrehiwot et al. (2010), and Kebede (2009). However, the conclusions of these studies have not shown consensus on the trends of flow. Conway and Hulme (1993) and Legesse et al. (2003) reported an increasing trend of the Blue Nile annual flow, whereas Bewket (2003), Gebrehiwot et al. (2010) and Kebede (2009) reported a decreasing trend of annual flow. Analysis of 40 years of flow data (i.e. from 1964 to 2003) by

* Corresponding author. Address: Tigray Agricultural Research Institute, P.O. Box 492, Tigray, Ethiopia. Tel.: +251 923022863.
E-mail address: dutg2006@yahoo.com (T.G. Gebremicael).

0022-1694/$ - see front matter © 2012 Elsevier B.V. All rights reserved.
http://dx.doi.org/10.1016/j.jhydrol.2012.12.023

Tesemma et al. (2010) showed no change of the annual flow from the Upper Blue Nile basin with the exception of an increase of the wet season flow. Several studies (e.g., Conway et al., 2004; Elshamy and Wheater, 2009) pointed out that the impact of climate change on the river flow is insignificant, whereas Ahmed (2010) and Taye and Willems (2012) showed the influence of climate to be uncertain. Taye and Willems (2012) showed that the high flow extremes of the Blue Nile are strongly influenced by climatic oscillations while the low flows are influenced by the combined effects of climate and landuse/land cover changes.

There are a handful of published studies that estimate annual sediment load from the Upper Blue Nile basin (e.g. Gordon, 2004; NBCBN, 2005; Steenhuis et al., 2009; Easton et al., 2010; and Betrie et al., 2011). These studies reported different results of sediment yield at the Upper Blue Nile outlet (El Diem gauging station), which range from 111×10^6 ton/year to 140×10^6 ton/year. To the authors' knowledge, however, no study was done to analyse the long-term trend of the sediment load.

The disagreements in the trends of flow and the amount of annual sediment load imply a limited understanding of the underlying causes. Therefore, the objectives of this study were to (i) assess the long-term variability of rainfall, runoff and sediment fluxes of the Upper Blue Nile using statistical methods, (ii) infer the causes of changes in runoff and sediment load as a function of landuse change derived from changes in the parameters of a physically based SWAT model, and (iii) check the consistency of the results from changes in flow and sediment fluxes as interpreted by changes of the SWAT model parameters against landuse change detected from remote sensing images of 28 years time difference.

The remainder of this paper is organized into four sections. Section 2 presents a brief description of the study area. Section 3 discusses the materials and methodology used in this study. Sections 4 and 5 present the results and conclusions of this study, respectively.

2. Description of study area

The Upper Blue Nile basin, locally called Abay, is located in the north-western part of Ethiopia as shown in Fig. 1. The topography of the basin is comprised of highlands and hills in the north-eastern part, and is dominated by valleys in the southern and western parts. The elevation varies from 480 m near the Sudanese/Ethiopian border to over 4200 m near the central part of the basin.

The climate of the basin is tropical highland monsoonal, with the majority of the rain falling from June to October. The average rainfall of the basin varies from 1000 mm/year in the north-east to above 2000 mm/year in south-east of the basin. Over 80% of its annual flow occurs from July to October and flows directly to the downstream countries (Sutcliffe and Parks, 1999).

The geology of the basin is mainly volcanic rocks and Precambrian basement rocks with small areas of sedimentary rock (Conway, 2000). The dominant soil types are 21% of Latosol and Alisols, 16% of Nitosols, 15% of Vertisols, and 9% of Cambisols (Betrie et al., 2011). The dominant land covers of the basin are savannah, dry land crop and pastures, grassland, crop and woodland, water body and sparsely vegetated plants (Ahmed, 2010).

3. Material and methodology

The null hypothesis of this study is that long-term landuse change in the Upper Blue Nile basin, if any, has no significant effect on runoff and sediment fluxes at the outlet. Accordingly, this paper focuses, first, on using statistical tests to detect trends of runoff and sediment fluxes at the basin outlet (i.e., El Diem station); next to infer possible causes by comparing the SWAT model parameters values for two different time periods, which are well apart temporally; and finally to verify those results by comparing two landuse maps of years 1973 and 2000.

3.1. Input data

The datasets used in this study include data related to soil, climate (e.g., rainfall and temperature), runoff, sediment, and landuse/cover maps. Long-term records of monthly data of rainfall, runoff, and sediment load were used for the statistical analysis. Daily climate, runoff, and sediment load data were used for the SWAT modelling. Satellite images (Landsat) of 1973 and 2000 were used to detect long-term landuse change.

The annual rainfall data from 1970 to 2005 of nine meteorological stations, as show in Fig. 2, were used to analyse long-term trends of rainfall over the Upper Blue Nile basin. Rainfall stations close to the headwaters of each tributary were selected. The monthly river discharge data from 1970 to 2009 and sediment concentrations data from 1980 to 2009 at El Diem station were used to assess seasonal and annual trends of flow and sediment fluxes, respectively. The observed daily data of flow and sediment load were used for SWAT model simulations.

The sediment concentration in the Blue Nile is measured only during the rainy season, which is from June to October and assumed to be negligible during the remaining months (Easton

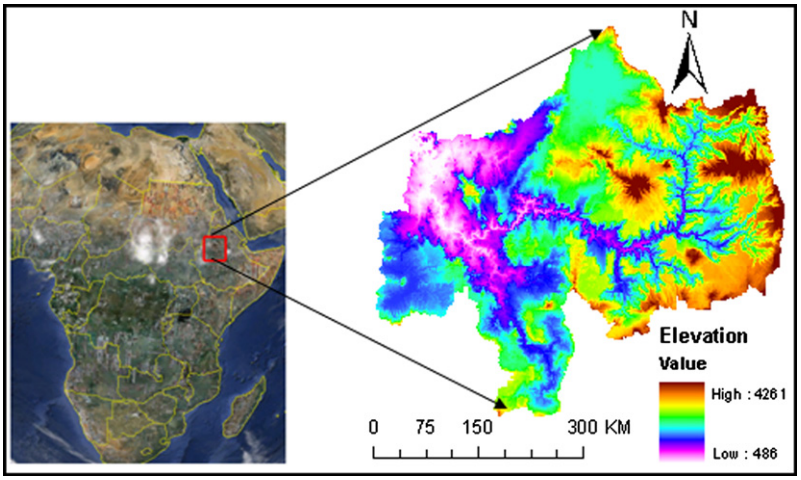

Fig. 1. Location map of the Upper Blue Nile basin.

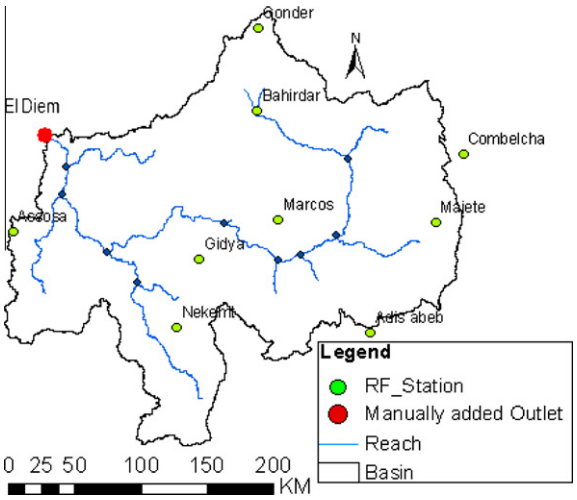

Fig. 2. Location of rainfall and discharge stations in Upper Blue Nile.

et al., 2010; Betrie et al., 2011). This is a realistic assumption given the extremely low concentration of the dry season. The observed sediment data were complete for the simulation period of 2000–2005. For the period of 1970–1976, however, observed sediment concentrations are available only from 1972 to 1973 with many missing values. To fill these missing data, it was assumed that the sediment concentration at El Diem is equal to the Roseires station for the given date. This assumption is realistic for three reasons (i) the two stations are 110 km apart and there is no significant inflow or abstraction in between; (ii) a linear regression was generated between the two stations and the regression slope (0.89) is not significantly different from 1 (Fig. 3). This explicitly indicates that the sediment concentrations at the Roseries and El Diem stations are similar. Furthermore, the correlation coefficient is high (0.88) indicating that a close relationship between the two stations. Therefore, the model of 2000s was calibrated from observed data, whereas the model of 1970s was calibrated using sediment data derived from the NBCBN rating curve. The NBCBN derived the sediment rating curve based on observed data during the early 1970s (NBCBN, 2005). Also, the sediment data generated from the rating curve were compared to the measured data in the year 1972 and 1973. This comparison showed good correlation (R^2 = 0.80).

The observed data for precipitation and temperature was obtained from 27 stations for daily rainfall and 19 stations for daily minimum and maximum temperature, respectively. The daily data were used to run the SWAT model for the simulation periods from

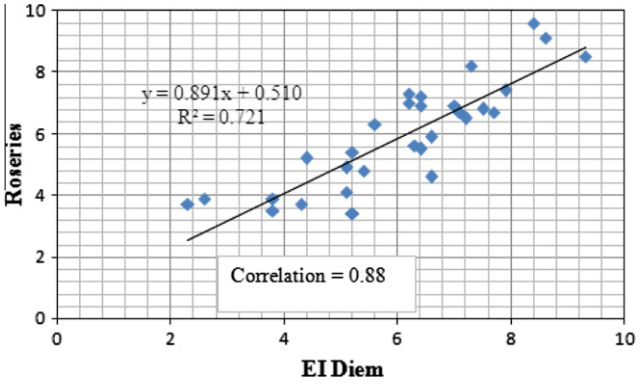

Fig. 3. Relationships between Roseries and El Deim daily sediment concentration (mg/L).

1970 to 1976, and 2000 to 2005. A weather generator model based on statistical summaries of long-term monthly means was used to generate the relative humidity, solar radiation and wind speed data from 18 stations within the basin.

3.2. Methodology

3.2.1. Statistical tests

The long-term trends of the hydrological and sediment fluxes were estimated using the non-parametric statistical tests of Mann–Kendall (MK) and Pettitt (Kendall, 1975; Lu, 2005; Pettitt, 1979; Zhang et al., 2008). The MK test is a rank based method for trend analysis of time series data (Burn et al., 2004; Tesemma et al., 2010). The normalized test statistics Z for the MK test is computed using Eqs. (1)–(3) below (Yu et al., 1993).

$$S = \sum_{i=1}^{n=1}\sum_{j=i+1}^{n} \mathrm{sgn}(x_j - x_i), \quad \text{where } \mathrm{sgn}(\theta) = \begin{cases} +1 \\ 0 \\ -1 \end{cases} \quad \text{if} \quad \begin{bmatrix} \theta > 0 \\ \theta = 0 \\ \theta < 0 \end{bmatrix} \tag{1}$$

$$Z = \begin{cases} \frac{S-1}{\sqrt{V(S)}} \\ 0 \\ \frac{S+1}{\sqrt{V(S)}} \end{cases} \quad \text{if} \quad \begin{bmatrix} S > 0 \\ S = 0 \\ S < 0 \end{bmatrix} \tag{2}$$

$$V(S) = \frac{1}{18}\left[n(n-1)(2n+5) - \sum_{t=1}^{m} t_i(t_i-1)(2t_i=5)\right] \tag{3}$$

where S is a MK statistic and V is variance.

First, the presence of monotonic increasing/decreasing trend was tested using the MK test. Second, the Pettitt test was applied to investigate the difference between cumulative distribution functions before and after a time instant. The significance of any trend in the dataset is provided in "*no trend*", "*an increasing or a decreasing trend*" designations based on defined confidence level (Lu, 2005). MK calculates Kendall's statistics (S), the sum of difference between data points and a measure of associations between two samples (Kendall's tau) to indicate increasing or decreasing trend. MK's Z statistics is normally distributed. Positive values of those parameters indicate a general tendency towards an increasing trend while negative values show a decreasing trend. Finally, a two-tailed probability (p-value) was computed and compared with the user defined significance level (5%) in order to identify the trend of variables. The Pettit test is a non-parametric test that requires no assumption about the distribution of the data and is used to identify if there is a point change in the data series (Pettitt, 1979). To avoid a false trend result, first the serial correlation of a time series should be investigated if it exists (Yue et al., 2002; Zhang et al., 2008). In this study, the trend-free pre-whitening (TFPW) method developed by Yue et al. (2002) was used to remove a serial correlation from time series if it exists (Burn et al., 2004).

The gradual trend test (i.e. MK), and abrupt change test (i.e. Pettitt) were employed on the seasonal and annual flow data series of 1970–2009 and the sediment load series of 1980–2009 at the outlet of the basin (El Diem station). Also, the seasonal and annual rainfall data series of nine stations were tested against the long-term trends.

3.2.2. SWAT modelling

A physically-based model, SWAT, was used to interpret the results of the statistical tests, and infer if the long-term trends are attributed to landuse changes. The SWAT model describes the relationship between inputs (e.g. rainfall), the system condition (e.g.

landuse/cover) and the outputs (e.g. flow and sediment load). Two independent SWAT simulations were performed from 1970 to 1976 and from 2000 to 2009. The difference between the values of the two model parameters could explain reasons for the envisaged trends of runoff and sediment fluxes (Tesemma et al., 2010).

SWAT is a conceptual, GIS interface tool that operates on a daily time step to envisage the impact of landuse and climate change on water, sediment and agricultural yields from large watersheds with varying soil, landuse and management practices over a certain period of time (Arnold et al., 1998; Neitsch et al., 2005). The model divides a basin into sub-basins and further into hydrological response units (HRUs) with a homogenous soil type, slope, landuse, and management practice (Arnold et al., 1998). The SWAT model computes surface runoff with two methods, the soil conservation service (SCS) curve number (CN) method (USDA, 1972) and the Green–Ampt infiltration method (Green and Ampt, 1911). The CN method was used in this study because of its capability to use daily input data (Arnold et al., 1998; Neitsch et al., 2005; Setegn, 2010; Betrie et al., 2011).

The SWAT model simulates the hydrology into land and routing phases. In the land phase, the amount of water, sediment and other non-point loads are calculated from each HRU and summed up to the level of sub-basins. Each sub-basin controls and guides the loads towards the basin outlet. The routing phase defines the flow of water, sediment and other non-point sources of pollution through the channel network to an outlet of the basin (Neitsch et al., 2005). SWAT computes soil erosion at a HRU level using the modified Universal Soil Loss Equation (MUSLE) (Wischmeier and Smith, 1978). This process constitutes computing sediment yields from each sub-basin and routing the sediment yields to the basin outlet. A detailed description of the hydrological and sediment components computation is available in the users' manual of SWAT model (e.g., Neitsch et al., 2005). Although SWAT provides three methods for estimating potential evapotranspiration, which are Penman–Monteith (Monteith, 1965), Priestly–Taylor (Priestley and Taylor, 1972), and Hargreaves methods (Hargreaves et al., 1985), the Hargreaves method was used in this study since it suits best for a basin with limited climatic data.

The SWAT model was built for two simulation periods (1970–1976 and 2000–2005). A Digital Elevation model (DEM), soil map, and landuse maps were used as inputs to SWAT. The DEM was obtained from the Global US Geological Survey site, and the landuse/cover maps were prepared from Landsat MSS and ETM + imageries (GLCC, 2010). The soil map was obtained from the global soil map of the Food and Agriculture Organization (FAO, 1995). It includes more than 500 soil types and has a spatial resolution of 10 km. The soil physical properties (e.g. bulk density, available water capacity, hydraulic conductivity, saturation hydraulic conductivity, particle-size distribution) were taken from Betrie et al. (2011). The landuse, soil and topography maps were overlaid to create a total number of 1553 HRUs over the Upper Blue Nile. The HRUs were selected by ignoring the landuse, soil and slope areas covering less than 5% of the total sub-basin area. This was necessary to reduce computation time of the model. The simulation period of the first model was from January 1, 1970 to December 31, 1976. The first year was used to warm-up the model, the years from 1971 to 1973 were used for the model calibration, and the years from 1974 to 1976 were used for the model validation. The simulation of the second model was performed from January 1, 2000 to December 31, 2005. The first 3 years (2000–2002) was used for the model calibration and the last 3 years (2003–2005) was used for the model validation. The two simulation periods (i.e., 1970–1976 and 2000–2005) were selected to detect landuse changes over a relatively long period. These periods were selected to include the period of high landuse changes of the 1980s (Zeleke and Hurni, 2001).

A sensitivity analysis was done to identify the most sensitive parameters of SWAT for the model calibration. In this study, latin-hypercube one factor at a time (LH-OAT) algorithm developed by van Griensven et al. (2006) and implemented as an automatic sensitivity analysis in the SWAT model was used to identify the most sensitive parameters. Next, the most sensitive parameters were automatically calibrated using sequential uncertainty fitting algorithm (SUFI-2), which is developed by Abbaspour et al. (2007). The model validation was done by running the same model for different simulation periods using a validation dataset as input. The model performance for the runoff and sediment load was then evaluated using statistical methods (Moriasi et al., 2007) such as Nash–Sutcliffe coefficient of efficiency (E), and coefficient of determination (R^2). Also, graphical comparisons of the simulated and observed data as well as water balance checks were used to evaluate the models performance. The coefficient of determination (R^2) describes the proportion of the total variance in the observed data that can be explained by the model (Legate and McCabe, 1999), which is shown by the following equation:

$$R^2 = \left[\frac{\left[\sum_i^n (Q_{m,i} - \overline{Q}_m) - (Q_{s,i} - \overline{Q}_s)\right]^2}{\sum_i^n (Q_{m,i} - \overline{Q}_m)^2 \sum_i^n (Q_{s,i} - \overline{Q}_s)^2}\right] \quad (4)$$

where $Q_{m,i}$ is the measured flow data in m^3/s or the sediment concentration in mg/l, $\overline{Q}_m$ is the mean n values of the measured data, $Q_{s,i}$ is the simulated flow data in m^3/s or the sediment concentration in mg/l, and $\overline{Q}_s$ is the mean n values of simulated data. The Nash–Sutcliffe coefficient of efficiency (E) has been widely used to evaluate the predictions of the SWAT model (Gassman et al., 2007; Betrie et al., 2011). E is defined as the ratio of residual variance to measured data variance (Nash and Sutcliffe, 1970) and calculated using Eq. (5). According to Moriasi et al. (2007) and Legate and McCabe (1999), model performance is accepted as satisfactory if $E > 0.5$ and $R^2 > 0.5$ for flow and sediment.

$$E = 1 - \left[\frac{\sum_i^n (Q_{m,i} - Q_{s,i})^2}{\sum_i^n (Q_{m,i} - \overline{Q})^2}\right] \quad (5)$$

After obtaining the best fitting parameters for runoff and sediment simulations from the early 1970s and late 2000s models, two different approaches were used to detect causes of runoff and sediment changes. First, parameters values for the two periods were compared assuming those values are not the same if landuse has changed in the basin. Second, the water balance results and the annual average sediment yields were compared.

3.2.3. Landuse map analysis

The third method of analysis is to detect landuse/cover change over the past 28 years to verify the results of the statistical tests and the SWAT model. Prior to classification and change detection, several pre-processing methods were implemented to prepare the landuse maps for two distinct periods. These include geometric correction, radiometric correction, topographic normalization and temporal normalization.

All scenes supplied by the EROS Data Centre were processed with the Standard Terrain Correction (Level 1T), which provides systematic radiometric and geometric accuracy for the imageries. However, in some parts of the study area there were significant discrepancies between the Landsat-1 MSS imageries and the underlying GIS base layers. The misaligned scenes were georectified to the underlying GLS 200 Geocover images by using a total of 38 control points and a Root Mean Square (RMS) error of less than 0.5 was achieved. The MSS data sets were resembled to a 30 m × 30 m pixel size using the nearest neighbour resembling

Table 1
Descriptions of the land cover classes identified.

S. no	Class name	Description
1	Rainfed cropland (RCL)	Area covered with temporary crops grown by rainfall
2	Grassland (GL)	Areas in which grasses are dominant
3	Wooded grassland (WGL)	Lands with herbaceous and tree canopy cover of 10–40%
4	Wood land (WL)	A single storey trees and exceed 5 m in height
5	Shrubs and bushes (SHB)	Low woody plant (<2 m) with multiple stems
6	Natural forest (NF)	Evergreen/deciduous broadleaf forest
7	Water body (WB)	Area covered with lakes, reservoirs, and ponds
8	Afro-alpine vegetation (AAV)	High altitude herbaceous and *Erica/Hypericum* forest
9	Barren land (BL)	Areas with little or no vegetation consisting of exposed soil/rocks
10	Irrigated crop land (ICL)	Area covered with temporary crops grown by irrigation
11	Plantation forest (PF)	Plantation of *Eucalyptus* globules and *Cupresus* spp.

technique in order to avoid altering the original pixel value of the image data (Jensen, 2005).

The original Digital Number (DN) was converted to at-satellite reflectance (Huang et al., 2002) using the Markham and Barker equations (Markham and Barker, 1986) in order to enhance the consistency landuse/cover characterization, remove relative radiometric noises, and minimize the cosine effect of different solar zenith angles among imageries, Atmospheric correction was not performed because the post-classification comparison approach adopted for landuse/cover change analysis also compensates for variation in atmosphere conditions between dates since each landuse/cover classification is independently classified (Song et al., 2001).

A hybrid supervised/unsupervised classification approach was carried out to classify the imageries of 1972/1973 (MSS) and 2000 (ETM+). First, Iterative Self-Organizing Data Analysis (ISODATA) clustering was performed to determine the spectral classes. ISODATA is an algorithm frequently used to determine the natural spectral groupings in a dataset for unsupervised classification (Tou and Gonzalez, 1974). Second, ground truth (i.e. reference data) was collected from already classified maps and in-depth interviews were held with local elders to associate the spectral classes with the cover types. Finally, a supervised classification was done using a maximum likelihood algorithm to extract nine landuse/cover classes from the 1972/1973 imageries and 11 classes from the 2000 imageries as presented in Table 1.

The accuracy of the classifications was assessed by computing the error matrix that compares the classification result with ground truth information. To assess the accuracy of thematic information derived from 1972/1973 (MSS) and 2000 (ETM+), the "design-based statistical inference" method was employed that provides unbiased map accuracy statistics (Jensen, 2005).

A total of 65 reference data were collected from old maps using stratified random sampling in order to assess the accuracy of the 1973 map. These reference data were assessed using the "confidence-building assessment" method. The confidence-building assessment method involves visual examination of the classified map by knowledgeable local elders to identify any gross errors. Similarly, in order to assess the accuracy of 2000 map, first unchanged land cover locations between 2000 and 2009 were identified by interviewing local elders and with the help of SPOT-5 (5 m resolution) 2007 imagery. Second, 294 ground truth data regarding land cover types and their spatial locations were collected from selected sample sites during the field campaign in 2009 using Global Positioning System (GPS). The number of samples required for each class was adjusted based on a proportion class and an inherent variability within each category. As there is no single universally accepted measure of accuracy, overall accuracy and kappa analysis were used to evaluate the accuracy of the classified maps. The overall accuracy was calculated by dividing the number of pixels classified correctly by the total number of pixels.

The post-classification change detection comparison was performed following Jensen's (2005) methodology. This was done to determine changes in landuse/cover between two independently classified maps from images of two different dates. Although this technique has some limitations, it is the most common approach as it does not require data normalization between two dates (Singh, 1989).

4. Results and discussion

In this section, the results of this study are presented and discussed. The results of the trend analysis of rainfall, runoff and sediment fluxes are presented in Section 4.1. Sections 4.2 and 4.3 present the results of the SWAT modelling and the landuse change detection, respectively.

4.1. Trend analysis results

The MK and Pettitt tests were applied to the annual rainfall pattern at nine stations in the Upper Blue Nile (locations are given in Fig. 2). The results of the MK test are presented in Table 2 including the shows station names, MK trend test, statistical summary (*S*), the computed *p*-value, and trend types. These results showed no change of annual rainfall for the last 36 years (1970–2005). All the computed probability values (*P*-values) except for Assosa were greater than the given significance level (5%). This result well agrees with earlier studies in the basin such as Conway (2000), Elshamy and Wheater (2009), and Tesemma et al. (2010). Those studies reported that there is no significant change of rainfall over the Upper Blue Nile during the last few decades although seasonal shifts could have occurred. This finding implies that inter-annual rainfall pattern is not the major driver for the trend changes of runoff and sediment fluxes in the Upper Blue Nile.

The trend analysis of the seasonal and annual stream flows as computed by the MK and Pettitt tests are summarized in Table 3

Table 2
Man-Kendall trend test and statistical summary of annual rainfall at nine stations in the Upper Blue Nile basin.

Station	Kendall's tau	*S*	*P*-value	Trend
Bahirdar	0.001	8	0.98	No significant change
Gonder	0.012	895	0.73	No significant change
Adiss Abeb	0.064	43	0.78	No significant change
Combelcha	0.017	1401	0.61	No significant change
Marcos	0.003	135	0.33	No significant change
Nekemt	−0.018	−335	0.72	No significant change
Majete	0.032	430	0.89	No significant change
Gidya	−0.043	−135	0.32	No significant change
Assosa	−0.078	−359	0.04	Significantly decreasing

Table 3
MK test results for the seasonal and annual flow and sediment load at El Diem Station.

	Season	Kendall's tau	*S*	*P*-value	Trend
Flow	Wet (June–September)	0.34	237	0.003	Significantly increasing
	Dry (October–February)	−0.37	−259	0.001	Significantly decreasing
	Short (March–May)	0.41	285	0.001	Significantly increasing
	Annual	0.25	175	0.028	Significantly increasing
Sediment load	Annual	0.7	200	<0.0001	Significantly increasing

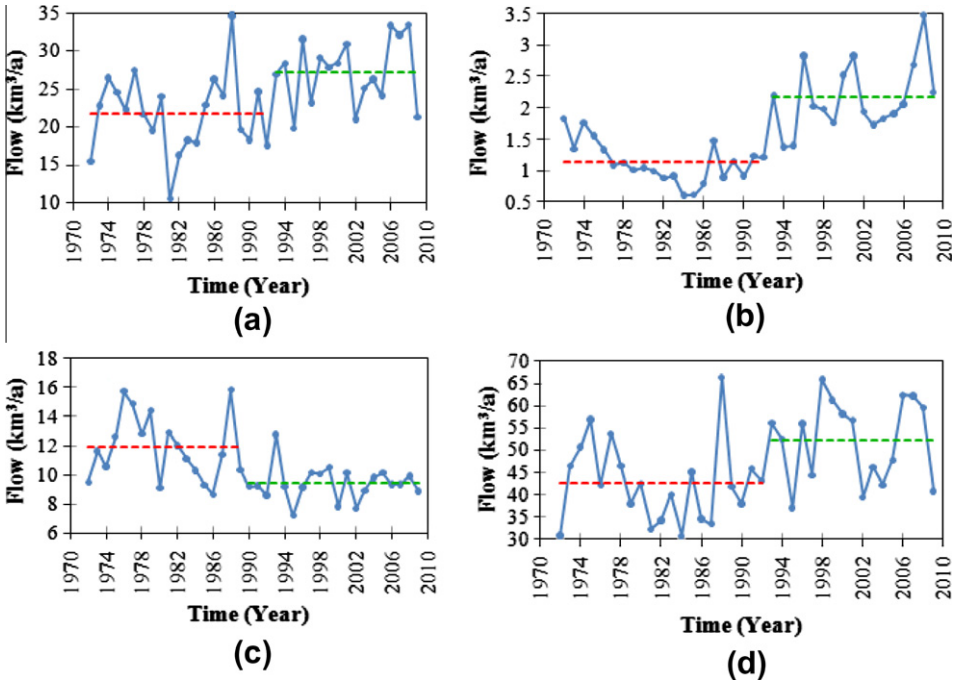

Fig. 4. The Pettitt homogeneity test of the seasonal and annual flows: (a) the wet season flow, (b) the short rainy season flow, (c) the dry season flow, and (d) the annual flow.

and Fig. 4, respectively. Table 3 shows Kendall's statistics (*s*), Kendall's tau, and computed probability (*p*-value). The MK results were given at a significance level of 5%. Fig. 4 shows the average of datasets before (red[1]) and after (green) a point change occurred. The results in Table 3 show a significant increasing trend of runoff during the wet season, the short rainy season, and the annual time period and a decreasing trend of stream flow during the dry season. These results were supported by the Pettitt test, which shows a significant abrupt upward change of stream flow as shown in Fig. 4. Most of these changes occurred in the early 1990s as shown in Fig. 4a and b. A significant abrupt downward change of the dry season stream flow occurred in 1979 as shown in Fig. 4c and d shows the increasing trend of the annual stream flow from the basin. To further validate these findings, the trend of annual flows at three key locations of the basin (i.e., Bahirdar, Kessi, and Dedessa) was analyzed using the above statistical tools (MK and Pettitt). The change point at Bahirdar and Kessie occurred in 1991–1992, which is consistent with Fig. 4, while at the Dedessa station, the change occurred 6 years later.

These results of the dry and wet season flows well agree with Tesemma et al. (2010), but the results of the short rainy season and annual flows do not agree. Tesemma et al. (2010) reported that the short rainy season and the annual flows are constant for the analysed period of 1964–2003, whereas this study (from 1970 to 2009) showed an increasing trend in both cases. However, we obtained similar results to Tesemma et al. (2010) for the same period of analysis (1964–2003). This difference is likely attributed to the last 6 years (2004–2009) that showed relatively higher discharges. Hence, it is interesting to note that the period of analysis is a critical factor to determine the given trends.

Since the rainfall over the basin during the 1970–2005 period has not shown significant changes (Table 2), the increasing trend of runoff from the Upper Blue Nile could be attributed to landuse change within the basin. A decreasing trend of the dry season flow (base flow) and an increasing trend of the wet season flow (peak flow), while the annual rainfall remained significantly unchanged, suggests a modification of catchment response that has led to an enhanced surface runoff from the Upper Blue Nile basin. The annual flow showed a significant increasing trend (Table 3), as both the wet and short rainy season flows increased more than that the base flow was reduced.

The trend of the sediment load at the basin outlet was examined using the MK and Pettitt statistical tests and the results indicated an increasing trend of sediment load between 1980 and 2009, as shown in the last row of Table 3. The MK test shows that the sediment load was significantly increased at a 5% significance level. The Pettitt test (Fig. 5) revealed that an increasing sediment load from 91×10^6 ton/year in 1980–1992 to 147×10^6 ton/year in 1993–2009.

To further confirm this result, the measured sediment concentrations in the 1970s and 2000s were compared and the

[1] For interpretation of color in Fig. 4, the reader is referred to the web version of this article.

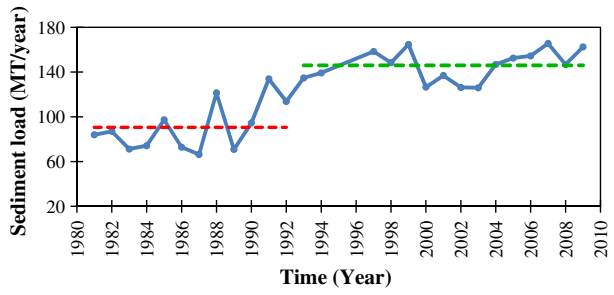

Fig. 5. The Pettitt homogeneity test of sediment load in the Upper Blue Nile during 1980–2009.

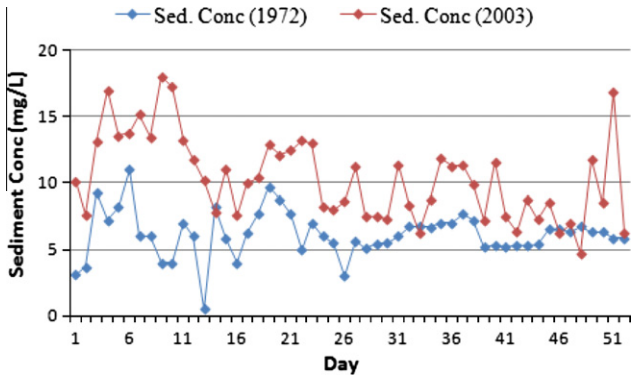

Fig. 6. Daily sediment concentration comparison between 1972 and 2003 rainy seasons.

comparison indicated that the concentrations has significantly increased, which implies an increasing of sediment load, as shown in Fig. 6. The increase of the sediment load by 61% during the past 30 years could be attributed to the modified runoff process associated with large-scale landuse change that exacerbated the soil erosion in the basin. Direct runoff is the only flow responsible for soil erosion and sediment transport in the stream (Steenhuis et al., 2009).

4.2. SWAT model results

The most sensitive parameters of the SWAT model that were used to simulate flow and sediment and their optimized values by the calibration process are presented in Table 4. Initial parameter estimates were taken from the default lower and upper bound values of the SWAT model database and from earlier studies in the basin (e.g. Easton et al., 2010; Betrie et al., 2011). The calibration parameters were derived for two independent models that were setup for the periods 1971–1973 and 2000–2002. Parameters such as SCS curve number (CN2), base flow alpha factor (ALPHA_BF), soil evaporation compensation factor (ESCO), threshold water depth in the shallow aquifer (GWQMN), channel effective hydraulic conductivity (CH_K2), ground water "revap" coefficient (GW_REVAP), surface runoff lag time (SURLAG), deep aquifer percolation fraction (RCHRG_DP), available water capacity (SOL_AWC), soil depth (SOL_Z), and ground water delay (GW_DELAY) were the most sensitive parameter for the flow predictions in the basin. Parameters including the linear re-entrainment parameter for channel sediment routing (SPCON), USLE support practice (USLE_P), and channel effective hydraulic conductivity (CH_K2) were among the most sensitive parameters for the sediment prediction.

Fig. 7 shows the calibration (Fig. 7a) and the validation (Fig. 7b) results of daily flow hydrographs for the simulation period 1971–1976. The model captured the daily runoff hydrographs both for the low and high flows. Model performance for the calibration period was $E = 0.80$ and $R^2 = 0.89$, and for the validation period $E = 0.78$ and $R^2 = 0.84$. The simulation results for the period 2000–2005 are given in Fig. 8. The model performance for the 2000–2005 period was $E = 0.84$ and $R^2 = 0.92$ for the calibration period, and for the validation period $E = 0.82$ and $R^2 = 0.88$. The performance of both models was satisfactory and agreed with previous studies in the basin. For instance, Easton et al. (2010) reported $E = 0.87$ and $R^2 = 0.92$ for calibration of daily flow and Betrie et al. (2011) $E = 0.68$ for calibration of daily flow at El Diem station.

The last column of Table 4 gives the percentage change of the calibrated model parameters for the simulation period of 2000–2002 relative to the simulation period of 1971–1973, which are periods after and before landuse change, respectively. A higher percentage change was obtained for some parameters as shown

Table 4
SWAT sensitive model parameters and their (final) calibrated values for 1971–1973 and 2000–2002 models.

Parameter	Description	Optimized parameter values		Change (%)
		1971–1973	2000–2002	
CN2[a]	Curve number	−0.17	−0.03	14
ALPHA_BF[b]	Base flow alpha factor	0.21	0.15	−28.6
ESCO[c]	Soil evaporation compensation factor	0.72	0.43	−67.3
CH_K2[b]	Channel effective hydraulic conductivity	16.32	17.54	7.5
GWQMN[c]	Thresh hold water depth in shallow aquifer Ground water "revap" coefficient	1002.25	823.54	−21.8
GW_REVAP[b]	Surface runoff lag time	0.12	0.17	41.7
SURLAG[b]	Deep aquifer percolation factor	6.35	4.68	−26.3
RCHRG_DP[b]	Available water capacity of soil	0.56	0.38	−32.1
SOL_AWC[a]	Maximum canopy storage	0.62	0.48	−22.6
CANMX[b]	Ground water delay	4.18	3.21	−23.2
GW_DELAY[b]	Linear re-entrainment parameter for channel sediment routing	78.16	72.96	−6.7
SPCON[a]		0.01	0.01	0
	USLE support practice	0.58	0.83	43.1
USLE_P[b]	Exponentiation re-entrainment parameter for channel sediment routing	1.2	1.32	10
SPEXP[b]				
HRU_SLP[b]	Average slope steepness	0.08	0.08	0
SLSUBBSN[a]	Average slope length	−0.35	−0.27	8
SOL_Z[a]	Soil depth	0.22	0.21	1

[a] Relative change in the parameters where value from SWAT database is multiplied by 1 plus a given range,
[b] Replace the initial parameter by the given value,
[c] Adding the given value to initial parameter value.

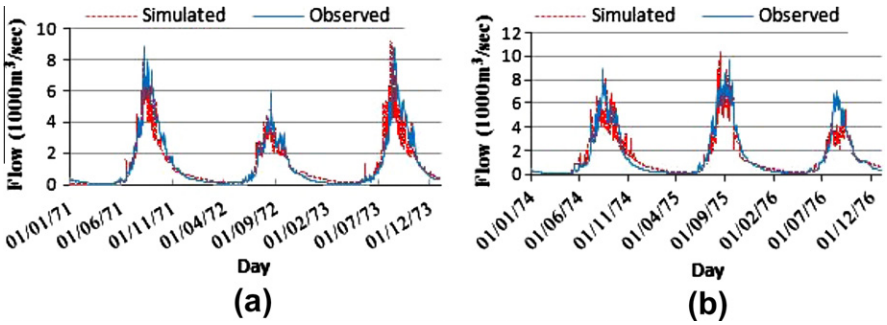

Fig. 7. Daily flow values for the 1971–1976 simulation period: (a) calibration and (b) validation.

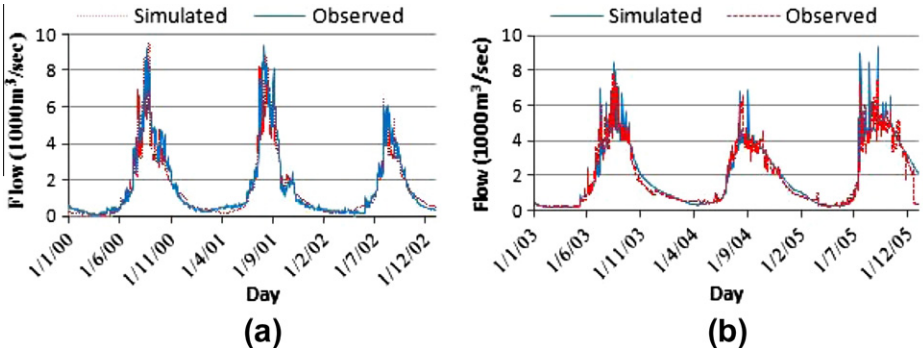

Fig. 8. Daily flow values for the 2000–2005 simulation period: (a) calibration and (b) validation.

in Table 4. According to Seibert and McDonnell (2010), such change indicates significant changes of the catchment response behaviour. The surface runoff response parameters (e.g. CN2, ESCO and SOL_AWC) showed a higher change. An increase in the CN2 value indicates that a higher amount of surface runoff was generated in the 2000s compared to the 1970s. The decrease of the ESCO value explains that more water was extracted from the lower soils to meet evaporative demand, which indicated a significant reduction of soil water. The available soil water capacity (SOL_AWC) was also significantly decreased for the past 35 years suggesting a shallower soil profile. A lower SOL_AWC implies the retention capacity of the soil is reduced and subsequently the surface runoff generation is increased.

Similarly, there was a clear change of subsurface response parameters (ALPHA_BF), threshold water depth in the shallow aquifer (GWQMN), ground water "revap" coefficient (GW_REVAP), deep aquifer percolation fraction (RCHRG_DP), and ground water delay (GW_DELAY) between the two periods. All changes indicated a quicker response towards surface runoff generation in the 2000s compared to the 1970s. ALPHA_BF is a direct index of ground water flow response to ground water recharge, and its lower value implies a smaller contribution of the base flow to the river discharge (Neitsch et al., 2005). The reduction of the GWQMN parameter means a decrease of the threshold value implying faster surface flow response. The deep aquifer percolation coefficient (RCHRG_DP), which controls the movement of water to the lower depth of the soil profile, showed a reduction. This indicates that less water percolates to the deep aquifer as compared to 1970s. Conversely, ground water "revap" coefficient that controls the movement of water between the soil profile and the shallow aquifer was increased. This may indicate that water from a shallow aquifer moves back to the overlying dry soils (unsaturated zone) during dry period (Neistche et al., 2005). As water is evaporated from capillary fringes, it is substituted by water from underlying aquifers.

The calibration results of the daily sediment loads at the El Diem station are displayed in Figs. 9 and 10. As is seen from Fig. 9, the magnitude and temporal variations of the simulated sediment load matches the observed sediment. The performance of the 1970–1976 model for simulating the daily sediment load is $E = 0.76$ and $R^2 = 0.78$ for the calibration period (Fig. 9a) and $E = 0.73$ and $R^2 = 0.75$ for the validation period (Fig. 9b). Similarly, the performance of the 2000–2005 model for simulating the sediment load is $E = 0.78$ and $R^2 = 0.75$ during calibration (Fig. 10a) and $E = 0.8$ and $R^2 = 0.72$ during the validation period (Fig. 10b). These results are comparable with model performances of earlier studies by Easton et al. (2010) and Betrie et al. (2011), who obtained $E = 0.74$ and $E = 0.88$, respectively. In addition to the above flow parameters which also affect the sediment fluxes, the value of USLE support practice (USLE_P) was significantly increased. This parameter expresses the anthropogenic influence on the physical process and a higher value of USLE_P indicates that there is a high soil loss in the watershed because of a poor management practice (USDA, 1972).

Next, the model results were checked using annual water and sediment balances. Table 5 presents the annual water balance components for the validation period. The average annual water balance of the basin shows that the surface runoff (Q_{surf}) contribution to the total river discharge has increased by 75%, while the subsurface flow (Q_{lat}) and the ground water (GW_Q) flow has decreased by 25% and 50%, respectively (see Table 5). Even with negligible change of rainfall between the two periods (1.3%), the total water yield at the outlet has increased by 25%. This clearly depicts a modification of catchment response and thus a possible change of the physical characteristics of the basin between 1970s and 2000s. The simulated results of the major components of the water balance match the observed values in the basin. It seems that the model has unrealistically over-predicted the deep aquifer recharge PERC (22%) compared to total yield (18.7%). SWAT considers PERC as a loss from the system, and does not contribute to the total yield

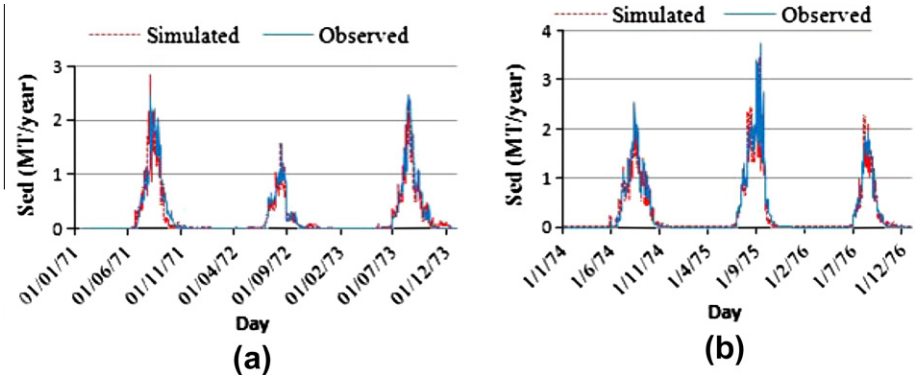

Fig. 9. Daily sediment load for the 1971–1976 simulation period: (a) calibration and (b) validation.

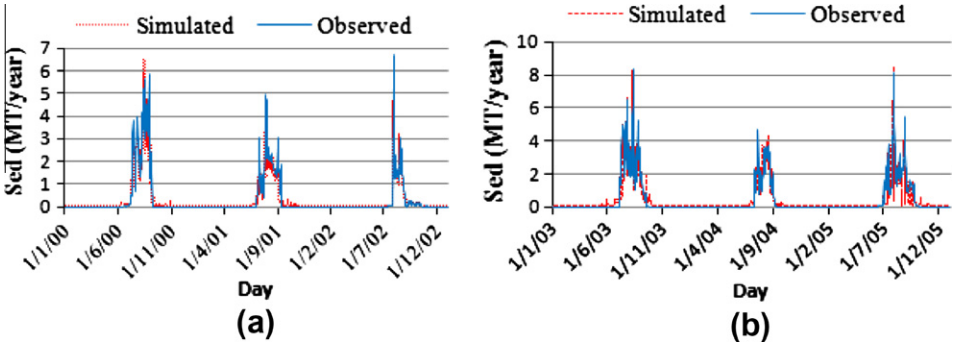

Fig. 10. Daily sediment load for the 2000–2005 simulation period: (a) calibration and (b) validation.

Table 5
The annual water balance of the Upper Blue Nile basin for the 1974–1976 and 2003–2005 validation periods.

Simulation period	Units	Rainfall	ET	Q_{surf}	Q_{lat}	GW_Q	Water yield	SW	PERC	TLosses
1974–1976	mm/year	1426	758	145	97	24	267	77	315	9
	%	100	53	10.3	6.8	2.4	18.7	5.4	22.1	0.64
2003–2005	mm/year	1445	774	254	73	12	332	97	220	12
	% a	100	54	18	5	1	24	7	15	1

Where ET is evapotranspiration, Q_{surf} is surface runoff, Q_{lat} is lateral flow, GW_Q is ground water flow, water yield is the total water yield ($Q_{surf} + Q_{Lat} + GW_Q$ – transmission losses), SW is soil water, and PERC is percolation (ground water recharge).

from the basin (Arnold et al., 1998; Neistche et al., 2005). This may not be realistic and the literature shows similar difficulties of estimating groundwater flow and deep ground water recharge using SWAT (Kalin and Hantush, 2006; Setegn et al., 2008). However, the uncertainty of the model on deep water recharge may have negligible effect in the conclusion of this study, assuming errors in both models can offset each other.

The annual average sediment load from the basin was 4.46 t/ha and 6.8 t/ha during the validation periods of 1974–1976 and 2003–2005, respectively. These results demonstrate that the total sediment yield from the basin has increased by 53% in the past 28 years. This could be due to the high sediment production and soil erosion rates from the basin.

Therefore, the results of the SWAT simulations supported the findings obtained from the statistical tests, namely that both runoff and sediment load from the Upper Blue Nile basin, showed an increasing trend during the last 28 years. Moreover, the comparisons of the SWAT model parameters for two simulation periods showed that the likely catchment response changes are attributed to increased surface runoff and reduced groundwater flow.

4.3. Landuse change detection

Table 6 and Fig. 11 depict landuse/cover change between the period 1973 and 2000. Note that the acronyms used in Table 6 are taken from Table 1. In 1973, the Upper Blue Nile basin was dominated by wooded grassland (26.9%), followed by rainfed cropland (26.5%), wood land (24.5%), and shrubs and bushes (12.2%). In 2000, on the other hand, the basin was dominated by rainfed cropland (47.9%), followed by wood land (16.9%), shrubs and bushes (11.1%), wooded grassland (10.6%), and grassland (8.9%). The areal coverage of rainfed cropland, grassland, water body and barren land showed a growth of 81%, 56%, 14% and 241%, respectively. On the other hand, wooded grassland, wood land, shrubs and bushes, natural forest, afro-alpine vegetation showed a decline by 61%, 31%, 8%, 51%, and 5%, respectively. Out of 83,691 km^2 of rainfed cropland observed in 2000, 30,213 km^2 (36%) remain unchanged, but 64% of it gained from other classes. The contribution of wooded grassland and wood land to the 81% growth of rainfed cropland was 34% and 20%, respectively. About 181 km^2 of wood land, 30 km^2 of wooded grassland, and 16 km^2 of shrubs and

Table 6
Transition matrix of landuse/cover change during the period 1973–2000.

Area (km^2) 1973 [a]	RCL	GL	WGL	WL	SHB	NF	WB	AAV	BL	Total	%
Area (km^2) 2000											
RCL	30213	5203	28724	17039	1061	1411	19.0	19.5	–	83,691	47.9
GL	6572	1025	4110	3449	146	232	6.8	–	–	15,541	8.9
WGL	3502	2234	7718	3312	1504	185	3.9	9.6	–	18,469	10.6
WL	5083	813	5358	17235	123	921	3.0	3.5	–	29,539	16.9
SHB	256	38	150	674	18353	0.1	–	–	–	19,471	11.1
NF	173	27	98	659	0.7	795	7.4	–	–	1759	1.0
WB	32	304	47	99.7	0.6	5.6	2991	–	–	3479	2.0
AAV	22	0.6	–	–	–	–	–	231.1	–	254	0.1
BL	63	2450	626	146	40.9	1.0	9.5	2.9	471	1605	0.9
ICL	8	–	30.1	181	16.4	–	–	–	–	235	0.1
PF	414	85.4	186	90.3	8.6	18.3	0.2	0.2	–	802	0.5
Total	46338	9974.2	47047	42886	21255	3569	3040	266.9	471	174,846	
Percent	26.5	5.7	26.9	24.5	12.2	2.0	1.7	0.2	0.3		
Change (%)	81	56	−61	−31	−8	−51	14	−5	241		

[a] See Table 1 for definition of acronyms.

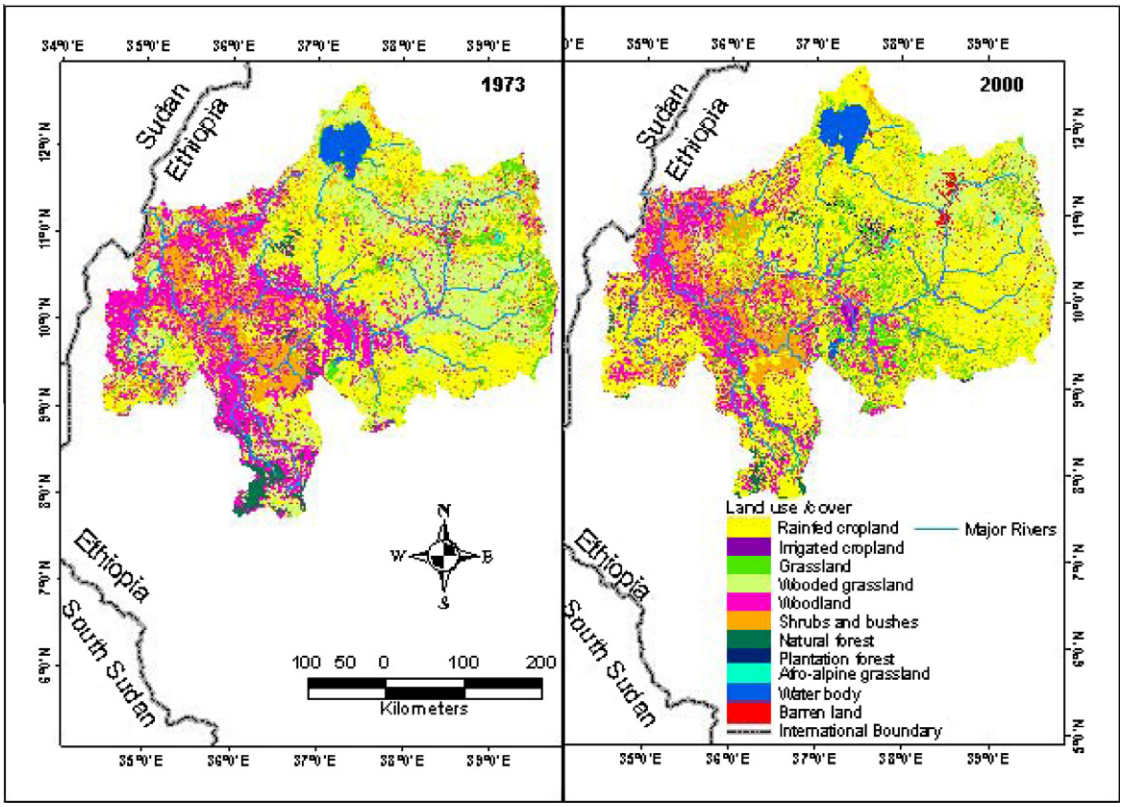

Fig. 11. Landuse/cover maps of the Upper Blue Nile basin in 1973 and 2000.

bushes were converted into irrigated cropland in 2000. This indicates a significant deforestation of the natural woody vegetation in order to have more cultivated land in the basin. However, 802 km^2 of plantation forest was observed in 2000 as a new land cover. This explains that previous deforestation has led the local people to plant trees as a mean to cope with the scarcity of fuel wood and other uses. This result well agrees with other local level studies (Zeleke and Hurni, 2001; Bewket, (2003); Legesse et al. (2003), Amsalu et al. (2007), Kebede (2009), and Teferi et al. (2010). These local studies reported the dramatic changes of the natural vegetation cover into the agricultural crop land.

The observed landuse change pattern, namely the deforestation of natural woody vegetation and the expansion of cultivated land, is consistent with the results from the statistical analysis (Section 4.1) and the interpretation of the SWAT model simulations (Section 4.2). It is therefore plausible that the observed increasing trends of surface runoff and sediment load from the Upper Blue Nile basin are caused by landuse change over a large area of the basin, and in particular by the conversion of the natural vegetation cover into the agricultural crop land.

5. Conclusions

The objectives of this study were to understand the long-term variations of hydrology and sediment fluxes of the Upper Blue Nile

Basin using statistical techniques (MK and Pettitt tests), and to interpret the results using a physically-based hydrological model (SWAT) and landuse/cover maps. The MK and Pettitt tests showed no statistically significant change of the annual rainfall over the Upper Blue basin between 1970s and 2000s. However, both tests showed a statistically significant increasing trend of runoff during the wet season (i.e., from June to September) and the short season (i.e., from March to May), and a decreasing trend of the dry season (i.e., from October to February) flow. The annual stream flow and the sediment load from the basin increased significantly for the past 39 years (1971–2009). The Pettitt test showed that most of these changes occurred in the early 1990s and that a significant abrupt downward change of dry season flow occurred around 1979. The results of the statistical tests also showed sensitivity to the time domain of the analysis.

The SWAT model was used to predict the daily runoff and the daily sediment load at the basin outlet (El Diem station, located at the Ethiopia-Sudan border). The null hypothesis was that the calibrated parameters of the model would be identical for two different time windows (1970s and 2000s). The modelling results showed that the model parameters, specifically the surface runoff and the groundwater parameters, were significantly different for the 1970s and 2000s simulation periods. These changes may be attributed to the modification of the basin physical characteristics. This was verified by comparing landuse maps of 1973 and 2000, which showed a significant conversion of natural landuse classes (forests, wood land and grass land) into agricultural crop and barren lands. The combined results from three different approaches, namely statistical tests, physically-based modelling and landuse change analysis, are consistent with the hypothesis that landuse change has modified the runoff generation process, which has caused the increasing trend of runoff and sediment load from the Upper Blue Nile basin during the last four decades.

These findings can be useful for basin-wide water resources management in the Blue Nile basin, as they not only provide insights on catchment behaviour aggregated at a basin scale, but also give a better understanding of embedded interdependencies between upstream and downstream areas and also at the transboundary level. However, this study does not cover other climate fluxes, nor does it consider the influence of long-term climatic cycles that could be important on the interpretation of the trend results. Therefore, it is recommended to further investigate the effect of the regional climate (e.g., multi-decadal oscillations) at different time spans and assess its impact on the runoff and sediment fluxes of the Upper Blue Nile.

Acknowledgements

The study was carried out as a project within a larger research program called "In search of sustainable catchments and basin-wide solidarities in the Blue Nile River Basin", which is funded by the Foundation for the Advancement of Tropical Research (WOTRO) of the Netherlands Organization for Scientific Research (NWO), and implemented by UNESCO-IHE, Addis Ababa University, the University of Khartoum and the Institute for Environmental Studies, VU Amsterdam.

References

Abbaspour, K., Yang, J., Maximov, I., Siber, R., Bogner, K., Mieleitner, J., Zobrist, J., Srinivasan, R., 2007. Modelling hydrology and water quality in the pre-alpine/alpine Thur watershed using SWAT. J. Hydrol. 333, 413–430.

Ahmed, S., 2010. Analysis of the Impact of Landuse Change and Climate Change on the Flows in the Blue Nile River Using SWAT. Katholieke Universiteit Leuven, Belgium, Leuven.

Amsalu, A.L., Stroosnijder, L., de Graaf, J., 2007. Long-term dynamics in land resource use and the driving forces in the Beressa watershed, highlands of Ethiopia. J. Environ. Manage. 83 (4), 448–459.

Arnold, J., Srinivasan, R., Muttiah, R., Williams, J., 1998. Large area hydrologic modeling and assessment part i: model development1. JAWRA 34, 73–89.

Betrie, G., Mohamed, Y., van Griensven, A., Srinivasan, R., Mynett, A., 2011. Sediment management modelling in Blue Nile Basin using SWAT model. Hydrol. Earth Syst. Sci. 7, 5497–5524.

Bewket, W., 2003. Towards integrated watershed management in highland Ethiopia: the Chemoga watershed case study. Trop. Resour. Manage. Pap. 44, 2003.

Burn, D., Cunderlik, J., Pietroniro, A., 2004. Hydrological trends and variability in the Liard River basin. Hydrol. Sci. J. 49, 53–68.

Conway, D., 2000. The climate and hydrology of the Upper Blue Nile River. Geogr. J. 166, 49–62.

Conway, D., Hulme, M., 1993. Recent fluctuations in precipitation and runoff over the Nile sub-basins and their impact on main Nile discharge. Clim. Change 25, 127–151.

Conway, D., Mould, C., Bewket, W., 2004. Over one century of rainfall and temperature observations in Addis Ababa, Ethiopia. Int. J. Climatol. 24, 77–91.

Easton, Z., Fuka, D., White, E., Collick, A., Asharge, B., McCartney, M., Awulachew, S., Ahmed, A., Steenhuis, T., 2010. A multibasin SWAT model analysis of runoff and sedimentation in the Blue Nile, Ethiopia. Hydrol. Earth Syst. Sci. 14, 1827–1841.

Elshamy, M., Wheater, H., 2009. Performance assessment of a GCM land surface scheme using a fine-scale calibrated hydrological model: an evaluation of MOSES for the Nile Basin. Hydrol. Process. 23, 1548–1564.

FAO, 1995. Digital Soil Map of the World and Derived Soil Properties. Food and Agriculture Organization of the United Nations, Rome, Italy.

Garzanti, E., And, S., Vezzoli, G., Ali Abdel Megid, A., El Kammar, A., 2006. Petrology of Nile River sands (Ethiopia and Sudan): sediment budgets and erosion patterns. Earth Planet. Sci. Lett. 252, 327–341.

Gassman, P.W., Reyes, M.R., Green, C.H., Arnold, J.G., 2007. The soil and water assessment tool: historical development, applications, and future research directions. Am. Soc. Agric. Biol. Eng. 50, 1211–1250.

Gebrehiwot, S., Taye, A., Bishop, K., 2010. Forest cover and stream flow in a headwater of the blue nile: complementing observational data analysis with community perception. AMBIO: J. Human Environ. 39, 284–294.

Global Land Cover Characterization (GLCC), 2010. <http://edcsns17.cr.usgs.gov/glcc/glcc.html> (last access 12.12.10).

Gordon, N., 2004. Stream Hydrology: An Introduction for Ecologists. John Wiley & Sons Inc..

Green, W., Ampt, G., 1911. Studies on soil physics, the flow of air and water through soils. J. Agric. Sci. 4, 1–24.

Hargreaves, G., Hargreaves, G., Riley, J., 1985. Agricultural benefits for Senegal River basin. J. Irrig. Drain. E – ASCE 111, 113–124.

Huang, C., Wylie, B., Yang, L., Homer, C., Zylstra, G., 2002. Derivation of a Tassled Cap transformation based on Landsat and at-satellite reflectance. Int. J. Remote Sens. 23, 1741–1748.

Hurni, H., 1993. In: Pimentel, D. (Ed.), Land Degradation, Famine, and Land Resource Scenarios in Ethiopia: World Soil Erosion and Conservation. Cambridge University Press, Cambridge, UK.

Hurni, H., Tato, K., Zeleke, G., 2005. The implications of changes in population, landuse, and land management for surface runoff in the upper Nile Basin Area of Ethiopia. Mount. Res. Develop. 25, 147–154.

Jensen, J.R., 2005. Introductory Digital Image Processing: A Remote Sensing Perspective, third ed. Prentice Hall, Upper Saddle River, NY, 526 pp.

Kalin, L., Hantush, M., 2006. Hydrologic modeling of an eastern Pennsylvania watershed with NEXRAD and rain gauge data. J. Hydrol. Eng. 11, 555–569.

Kebede, E., 2009. Hydrological Responses to Land Cover Changes in Gilgel Abbay Catchment of Ethiopia. ITC, The Netherlands.

Kendall, M., 1975. Rank Correlation Methods. Charles Griffin, London.

Legate, D., McCabe, J., 1999. Evaluating the use of goodness-of-fit measures in hydrologic and hydro-climatic model validation. Water Resour. Res. 35 (1), 233–241.

Legesse, D., Vallet-Coulomb, C., Gasse, F., 2003. Hydrological response of a catchment to climate and landuse changes in Tropical Africa: case study South Central Ethiopia. J. Hydrol. 275, 67–85.

Lu, X., 2005. Spatial variability and temporal change of water discharge and sediment flux in the Lower Jinsha tributary: impact of environmental changes. River Res. Appl. 21, 229–243.

Markham, B.L., Barker, J.L., 1986. Landsat MSS and TM post calibration dynamic ranges, exoatmospheric reflectances and at satellite temperatures. EOSAT Landsat Tech. Notes 1, 3–8.

Monteith, J.L., 1965. Evaporation and environment. Symp. Soc. Exp. Biol. 19, 205–234.

Moriasi, D., Arnold, J., Van Liew, M., Bingner, R., Harmel, R., Veith, T., 2007. Model evaluation guidelines for systematic quantification of accuracy in watershed simulations. Am. Soc. Agric. Biol. Eng. 50 (3), 885–890.

Nash, J., Sutcliffe, J., 1970. River flow forecasting through conceptual models part I – A discussion of principles. J. Hydrol. 10, 282–290.

NBCBN, 2005. Survey of Literature and Data Inventory in Watershed Erosion and Sediment Transport. Nile basin Capacity Buliding Network, Cairo.

Neitsch, S.L., Arnold, J.G., Kiniky, J.R., Williams, J.R., 2005. Soil and Water Assessment Tool Technical Documentation: Version 2005, United States Department of Agriculture, Agricultural Research Service.

Pettitt, A., 1979. A non-parametric approach to the change-point problem. Appl. Stat. 28, 126–135.

Priestley, C., Taylor, R., 1972. On the assessment of surface heat flux and evaporation using large-scale parameters. Mon. Weather Rev. 100, 81–92.

Seibert, J., McDonnell, J.J., 2010. Land-cover impacts on streamflow: a change-detection modeling approach that incorporates parameter uncertainty. Hydrol. Sci. J. 55 (3), 316–332.
Setegn, S., 2010. Modelling the Hydrological and Hydrodynamic Processes in Lake Tana Basin, Ethiopia, Ph.D. Thesis, TRITA-LWR, KTH, Sweden.
Setegn, S., Srinivasan, R., Dargahi, B., 2008. Hydrological modelling in the Lake Tana Basin, Ethiopia using SWAT model. Open Hydrol. J. 2, 49–62.
Singh, A., 1989. Digital change detection techniques using remotely sensed data. Int. J. Remote Sens. 10, 989–1003.
Song, C., Woodcock, C.E., Seto, K.C., Lenney, M.P., Macomber, S.A., 2001. Classification and change detection using Landsat TMdata: when and how to correct atmospheric effects? Rem. Sens. Environ. 75, 230–244.
Steenhuis, T.S., Collick, A.S., Easton, Z.M., Leggesse, E.S., Bayabil, H.K., White, E.D., Awulachew, S.B., Adgo, E., Ahmed, A.A., 2009. Predicting discharge and sediment for the Abay (Blue Nile) with a simple model. Hydrol. Process. 23, 3728–3737.
Sutcliffe, J., Parks, Y., 1999. The Hydrology of the Nile. IHAS Special Publication No.5. Int. Hydrol. Sci., Wallingford, UK.
Taye, M.T., Willems, P., 2012. Influence of climate variability on representative QDF predictions of the upper Blue Nile Basin. J. Hydrol. 411, 355–365.
Teferi, E., Uhlenbrook, S., Bewket, W., Wenninger, J., Simane, B., 2010. The use of remote sensing to quantify wetland loss in the Choke Mountain range, Upper Blue Nile basin, Ethiopia. Hydrol. Earth Syst. Sci. 14, 2415–2428.
Tesemma, Z.K., Mohamed, Y.A., Steenhuis, T.S., 2010. Trends in rainfall and runoff in the Blue Nile Basin: 1964–2003. Hydrol. Process. 24, 3747–3758.
Tibebe, D., Bewket, W., 2010. Surface runoff and soil erosion estimation using the SWAT model in the Keleta Watershed, Ethiopia. Land Degrad. Develop.. http://dx.doi.org/10.1002/ldr.1034.
Tou, J.T., Gonzalez, R.C., 1974. Pattern Recognition Principles. Addison-Wesley, London.
USDA, 1972. USDA Soil Conservation Service. National Engineering Handbook, Section 4.
Van Griensven, A., Meixner, T., Grunwald, S., Bishop, T., Diluzio, M., Srinivasan, R., 2006. A global sensitivity analysis tool for the parameters of multi-variable catchment models. J. Hydrol. 324, 10–23.
Wischmeier, W.H., Smith, D.D., 1978. Predicting Rainfall Erosion Losses: A Guide to Conservation Planning. Agricultural Handbook No. 537. US Department of Agriculture, Washington, DC, pp. 1–58.
Yu, Y.-S., Zou, S., Whittemore, D., 1993. Non-parametric trend analysis of water quality data of rivers in Kansas. J. Hydrol. 150, 61–80.
Yue, S., Pilon, P., Phinney, B., Cavadias, G., 2002. The influence of autocorrelation on the ability to detect trend in hydrological series. Hydrol. Process. 16, 1807–1829.
Zeleke, G., Hurni, H., 2001. Implications of landuse and land cover dynamics for mountain resource degradation in the northwestern Ethiopian highlands. Mount. Res. Develop. 21, 184–191.
Zhang, S., Lu, X.X., Higgitt, D.L., Chen, C.-T.A., Han, J., Sun, H., 2008. Recent changes of water discharge and sediment load in the Zhujiang (Pearl River) Basin, China. Global Planet. Change 60, 365–380.